Supporting information for: On the Stability and Morphology of Complex Coacervate Core Micelles: From Spherical to Worm-Like Micelles

Hanne M. van der Kooij,[*,†] Evan Spruijt,[†] Ilja K. Voets,[‡] Remco Fokkink,[†] Martien A. Cohen Stuart,[†] and Jasper van der Gucht[*,†]

Laboratory of Physical Chemistry and Colloid Science, Wageningen University, Dreijenplein 6, 6703 HB Wageningen, The Netherlands, and Institute for Complex Molecular Systems and Laboratory of Macromolecular and Organic Chemistry, Eindhoven University of Technology, P.O. Box 513, 5600 MB Eindhoven, The Netherlands

E-mail: hanne.vanderkooij@wur.nl; jasper.vandergucht@wur.nl

[*]To whom correspondence should be addressed

[†]Laboratory of Physical Chemistry and Colloid Science, Wageningen University, Dreijenplein 6, 6703 HB Wageningen, The Netherlands

[‡]Institute for Complex Molecular Systems and Laboratory of Macromolecular and Organic Chemistry, Eindhoven University of Technology, P.O. Box 513, 5600 MB Eindhoven, The Netherlands

Light scattering titration of PM2VP$_{41}$-*b*-PEO$_{204}$ with PAA$_{162}$

Lindhoud et al. and Brzozowska et al. have reported that C3Ms formed from PAA$_{139}$ and PM2VP$_{41}$-*b*-PEO$_{204}$ are most stable around pH 7 and $f_+ = 0.5$.[S1,S2] f_+ is here defined as follows:

$$f_+ = \frac{[n_+]}{[n_+] + [n_-]} \tag{1}$$

where $[n_+]$ and $[n_-]$ are the number concentrations of positively and negatively chargeable monomers, respectively. To verify that a 1 : 1 ratio of PM2VP to PAA monomers gives most stable C3Ms at pH 7.1, we have performed a dynamic light scattering titration of PM2VP$_{41}$-*b*-PEO$_{204}$ with PAA$_{162}$. The light scattering intensity, normalized by the total polymer concentration (I/C_p), and hydrodynamic radius of the C3Ms are plotted in Figure S1 as a function of f_+. We indeed find a maximum in both I/C_p and R_h around $f_+ = 0.5$. Since the position of this maximum is likely to be independent of the PAA and PM2VP length, we have used $f_+ = 0.5$ for all combinations of PAA$_m$ and PM2VP$_n$-*b*-PEO$_o$.

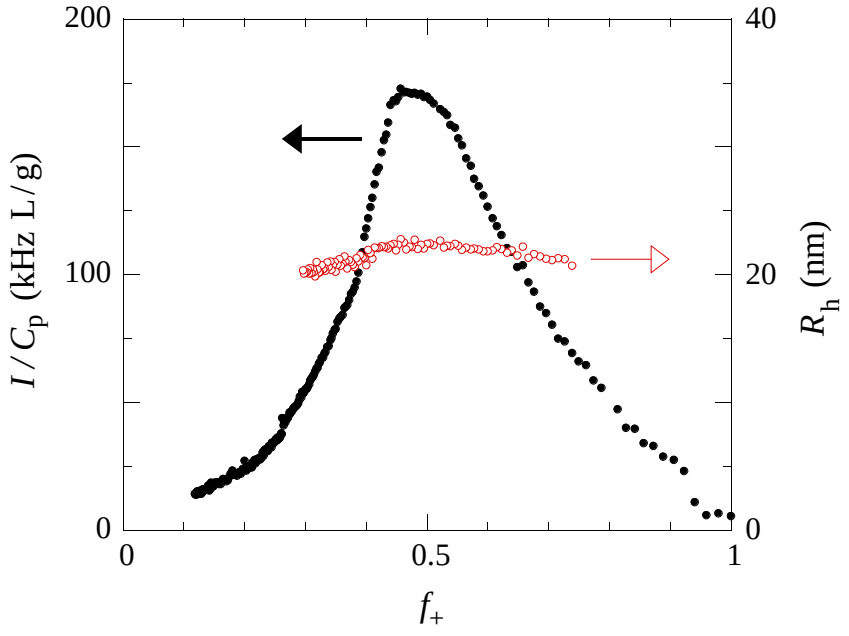

Figure S1: Light scattering intensity, normalized by the total polymer concentration, and hydrodynamic radius versus f_+ for a titration of 0.50 g/L PM2VP$_{41}$-*b*-PEO$_{204}$ with 1.0 g/L PAA$_{162}$, both at c_s = 10 mM and pH 7.1 ± 0.2. C_p ranged between 0.50 g/L ($f_+ = 1.0$) and 0.68 g/L ($f_+ = 0.12$).

Determination of $c_{s,cr}$ from a light scattering salt titration curve

Figure S2 shows how we estimate the critical salt concentration from a light scattering salt titration curve (see main text). We choose the intensity curve of $PAA_{20}/PM2VP_{41}$-*b*-PEO_{204} as an example, because it has a clear breakpoint. In this example, the 'baseline intensity' I_b = 2.4 kHz/mM. The critical salt concentration, i.e., the highest salt concentration for which the average I/c_{AA} of three subsequent points is larger than $2I_b$, is 0.27 M. If we used a threshold of $3I_b$, this would give $c_{s,cr}$ = 0.26 M, hence we estimate the error as 0.27 – 0.26 = 0.01 M.

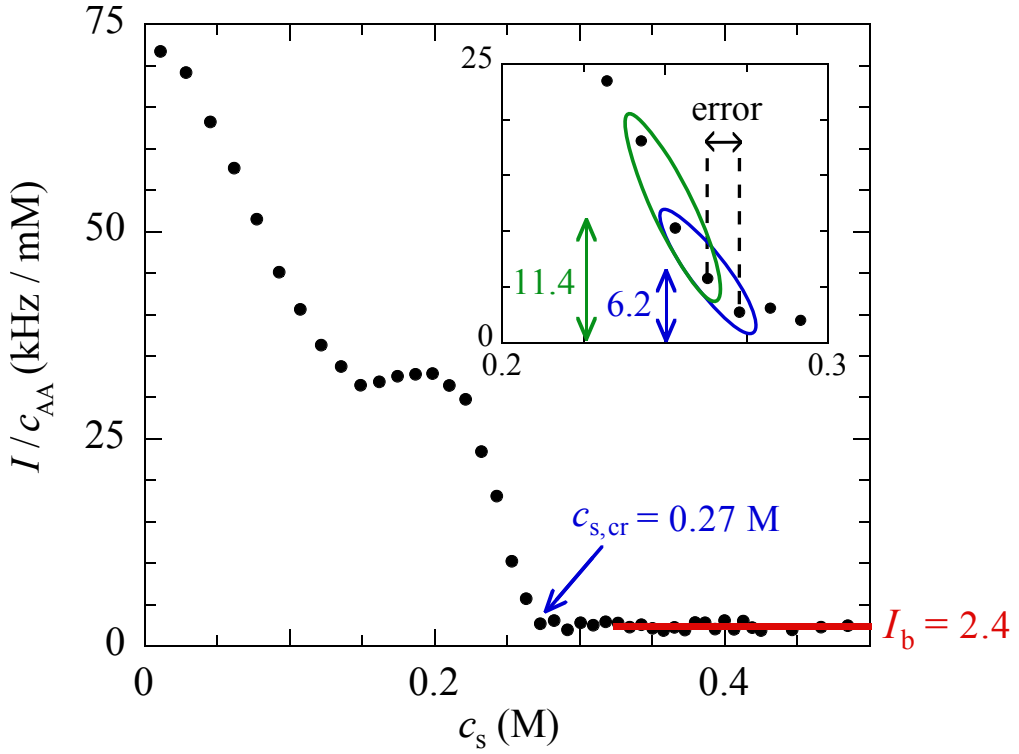

Figure S2: Light scattering intensity, normalized by the acrylic acid monomer concentration, versus salt concentration for a mixture of PAA_{20} and $PM2VP_{41}$-*b*-PEO_{204}. c_{AA} ranged from 1.1 mM at c_s = 0.01 M to 0.57 mM at c_s = 0.48 M. The numbers without units are in kHz/mM. The average I/c_{AA} of the three blue-circled points = 6.2 kHz/mM > $2I_b$, hence $c_{s,cr}$ = 0.27 M. The average I/c_{AA} of the three green-circled points = 11.4 kHz/mM > $3I_b$, hence the error is 0.27 – 0.26 M = 0.01 M.

Reversibility of response of PAA_{1728}/$PM2VP_{41}$-*b*-PEO_{204} to salt

Figure S3 shows the combined results of a light scattering salt and dilution titration for a mixture of PAA_{1728} and $PM2VP_{41}$-*b*-PEO_{204}. The normalized scattering intensity (a), mean apparent hydrodynamic radius (b), and critical salt concentration ($c_{s,cr}$ = 0.45 M) are approximately the same in both titrations, from which we conclude that the C3Ms respond reversibly to the salt concentration. These results provide evidence that our C3Ms are in or close to thermodynamic equilibrium.

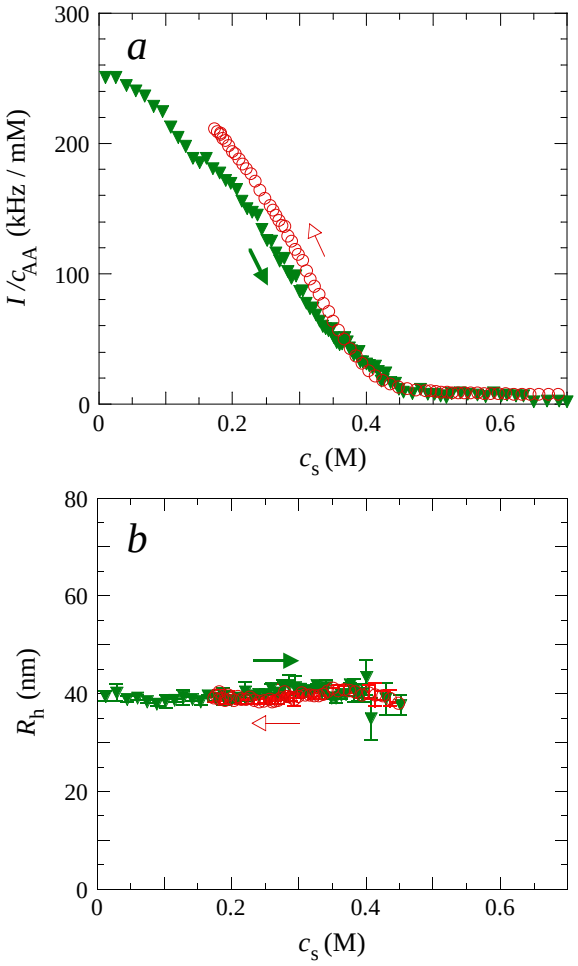

Figure S3: Salt and dilution titration curves for a mixture of PAA_{1728} and $PM2VP_{41}$-*b*-PEO_{204}. (a) Light scattering intensity, normalized by the acrylic acid monomer concentration, and (b) mean apparent hydrodynamic radius, as a function of salt concentration. The arrows indicate the direction of the titration. The symbols are averages of four independent runs. In (b), only data points up to the critical salt concentration are shown, with the error bars representing the standard deviations. In the salt titration, c_{AA} ranged from 4.4 mM at c_s = 0.01 M to 1.4 mM at c_s = 0.70 M. In the dilution titration, c_{AA} ranged from 4.4 mM at c_s = 0.70 M to 1.1 mM at c_s = 0.17 M.

Determination of critical PAA lengths from Figure 2a (main text)

To determine the critical PAA lengths of the three diblock copolymers, we have fitted two types of trendlines to the data in Figure 2a of the main text: horizontal trendlines to the hydrodynamic radii that are independent of N_{PAA}, and power-law trendlines to the radii that increase with increasing N_{PAA}. For PM2VP$_{128}$-*b*-PEO$_{477}$ and PM2VP$_{249}$-*b*-PEO$_{134}$, we have determined the critical PAA length from the intersection between these trendlines, which gives $N_{\mathrm{cr}} = 1.4 \times 10^3$ and 3.5×10^3, respectively. For PM2VP$_{41}$-*b*-PEO$_{204}$, however, the choice which points to include in the power-law trendline is ambiguous. We have therefore fitted *two* power-law trendlines: one to the four points with $N_{\mathrm{PAA}} \geq 1728$ and one to the three points with $N_{\mathrm{PAA}} \geq 4200$. The intersection points of these trendlines with the corresponding horizontal trendline are at $N_{\mathrm{PAA}} = 1.5 \times 10^3$ and 2.3×10^3. In Figure 2a of the main text, we show an 'average' of these two power-law trendlines, which passes through their common point and intersects the horizontal trendline at $\frac{2.3-1.5}{2} \times 10^3 = 1.9 \times 10^3 = N_{\mathrm{cr}}$. We have estimated the error in N_{cr} as $(2.3 - 1.9) \times 10^3 = 0.4 \times 10^3$.

Effect of salt on the CMCs of PAA_{13}/PM2VP$_{41}$-*b*-PEO_{204} and PAA_{139}/PM2VP$_{41}$-*b*-PEO_{204}

Figure S4 shows the effect of salt on the critical micelle concentrations of PAA_{13}/PM2VP$_{41}$-*b*-PEO_{204} and PAA_{139}/PM2VP$_{41}$-*b*-PEO_{204}. We have determined these CMC values by performing light scattering salt titrations for different initial polymer concentrations, and using the fact that c_{AA} at $c_{s,cr}$ equals the CMC at that salt concentration. Following the example of Wang et al.,[S3] we have fitted these data by a single-exponential dependence on the square root of the salt concentration. Clearly, the dependence of $c_{s,cr}$ on c_{AA} becomes negligible for high polymer concentrations. We also notice that this dependence seems to decrease with increasing PAA length. Since $N_{PAA} = 13$ is the smallest PAA length in our experiments, we believe that we can reliably neglect concentration effects for all the C3Ms we have studied.

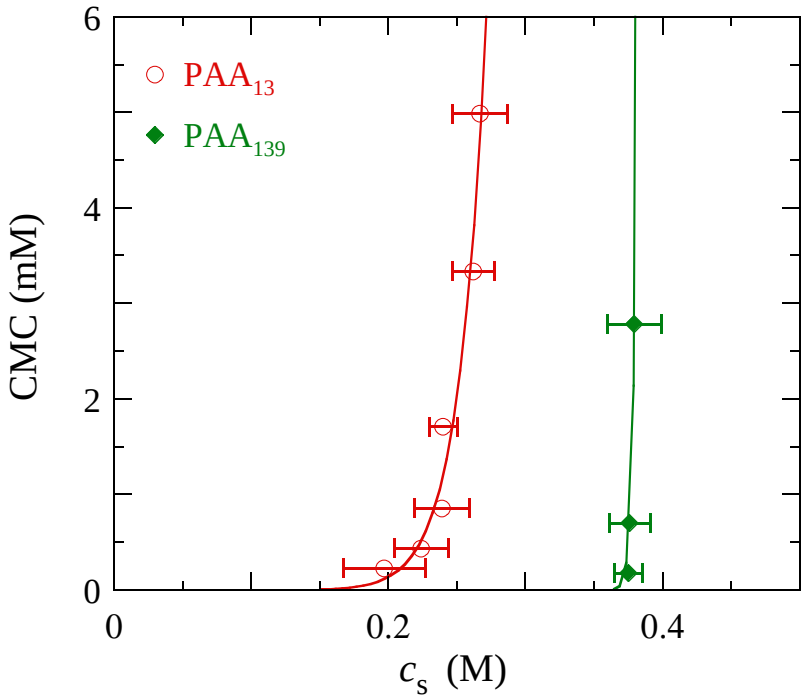

Figure S4: Critical micelle concentrations of C3Ms of PM2VP$_{41}$-*b*-PEO_{204} and PAA_{13} or PAA_{139} as a function of salt concentration. Symbols are experimentally determined CMC values. Solid lines are best-fit exponential dependences of the CMC on the square root of the salt concentration. Error bars represent the estimated error in the critical salt concentrations, as described in the Experimental details of the main text.

Estimation of the length of the worm-like micelles from D_r

To calculate the length of the worm-like micelles from their rotational diffusion coefficient (D_r), we have approximated the micelles as rigid spherocylinders, i.e., cylinders capped with hemispheres at both ends. The rotational diffusion coefficient of such structures can be expressed as a function of their average length (L) and diameter (d) according to:[S4]

$$D_r = \frac{3k_B T}{\pi \eta L^3}(\ln(L/d) + X_r(L/d)) \tag{2}$$

where η is the solvent viscosity and $X_r(L/d)$ is an empirical shape function, which takes the form for rigid spherocylinders:

$$X_r(L/d) = -0.372093 - \frac{0.95622}{\sqrt[4]{L/d}} + \frac{1.24792}{\sqrt{L/d}} + \frac{1.23085}{L/d} - \frac{1.99498}{(L/d)^2} + \frac{1.84201}{(L/d)^3} - \frac{0.664147}{(L/d)^4} \tag{3}$$

Fitting of scattering curves

The scattering curves in Figure 7 of the main text were fitted to form factor models included in the SASfit software package.[S5] These models are described in detail in the SASfit manual.[S6] The combined SLS and SAXS data of PAA_{13}/$PM2VP_{41}$-*b*-PEO_{204} at c_s = 10 mM and those of PAA_{139}/$PM2VP_{41}$-*b*-PEO_{204} at c_s = 280 mM were fitted to a form factor of a polydisperse core-shell sphere ('ExpShell'). This form factor consists of two contributions: (1) a monodisperse spherical core with radius R_c and uniform scattering length density η_c, and (2) a polydisperse (Gaussian distribution) spherical shell with thickness ΔR and a scattering length density η_{exp} that decreases exponentially between R_c and $R_c + \Delta R$. The best-fit parameters are shown in Table S1. The SAXS data of PAA_{13}/$PM2VP_{41}$-*b*-PEO_{204} at c_s = 180 mM were fitted to a form factor of a polydisperse (Gaussian distribution) flexible cylinder ('WormLikeChainEXV'). The best fit was obtained for a cross-sectional radius (R) of 1.5 ± 0.4 nm, a Kuhn length ($l = 2l_p$) of 44 nm, a contour length (L) of 280 nm, and a forward scattering (S_0) of 0.24×10^{10} cm^{-2}.

Table S1: Fitting parameters for the combined SLS and SAXS curves of (a) PAA_{13}/$PM2VP_{41}$-*b*-PEO_{204} at c_s = 10 mM and (b) PAA_{139}/$PM2VP_{41}$-*b*-PEO_{204} at c_s = 280 mM, shown in Figure 7 of the main text. A description of the parameters and the form factor model ('ExpShell') is given in the SASfit manual.

Sample	R_c (nm)	ΔR (nm)	α (-)	ϕ_{in} (-)	ϕ_{out} (-)	η_c ($\times 10^{10}$ cm^{-2})	η_{sh} ($\times 10^{10}$ cm^{-2})	η_{sol} ($\times 10^{10}$ cm^{-2})
a	5.0	3.7 ± 2.5	−0.9	0	1	9.52	9.52	9.34
b	3.4	2.0 ± 3.4	−3.6	0	1	9.54	9.54	9.40

SLS data for critical scattering analysis

Figure S5 shows the normalized Rayleigh ratio ($R(q)/Kc_{\mathrm{AA}}$) as a function of q^2 for mixtures of PAA_{13} and $\mathrm{PM2VP}_{41}$-*b*-PEO_{204} at five different salt concentrations. To estimate $R(0)/Kc_{\mathrm{AA}}$ at each salt concentration, the data points in the range $0.17 < q^2 < 0.46 \times 10^{10}$ cm^{-2} were linearly extrapolated to $q^2 = 0$. In Figure 8 of the main text, $R(0)/Kc_{\mathrm{AA}}$ is plotted as a function of the separation from the critical salt concentration ($c_{\mathrm{s,cr}} - c_{\mathrm{s}}$).

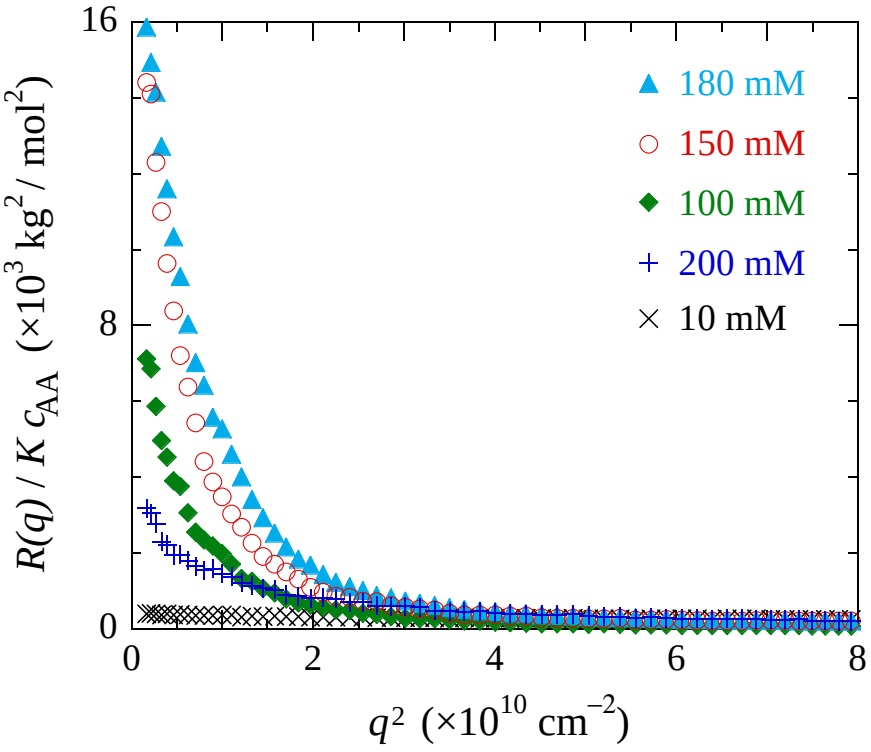

Figure S5: Analysis of critical scattering from C3Ms of PAA_{13} and $\mathrm{PM2VP}_{41}$-*b*-PEO_{204}. The normalized Rayleigh ratio is plotted as a function of q^2 for five different salt concentrations, as indicated by the labels. The polymer concentration (c_{AA}) ranged from 4.4 mM at c_{s} = 10 mM to 3.6 mM at c_{s} = 200 mM.

References

(S1) Lindhoud, S.; de Vries, R.; Schweins, R.; Cohen Stuart, M. A.; Norde, W. Salt-induced release of lipase from polyelectrolyte complex micelles. *Soft Matter* **2009**, *5*, 242–250.

(S2) Brzozowska, A.; Hofs, B.; de Keizer, A.; Fokkink, R.; Cohen Stuart, M.; Norde, W. Reduction of protein adsorption on silica and polystyrene surfaces due to coating with complex coacervate core micelles. *Colloids and Surfaces A: Physicochemical and Engineering Aspects* **2009**, *347*, 146–155.

(S3) Wang, J.; de Keizer, A.; Fokkink, R.; Yan, Y.; Cohen Stuart, M. A.; van der Gucht, J. Complex coacervate core micelles from iron-based coordination polymers. *The Journal of Physical Chemistry B* **2010**, *114*, 8313–8319.

(S4) Aragon, S. R.; Flamik, D. High precision transport properties of cylinders by the boundary element method. *Macromolecules* **2009**, *42*, 6290–6299.

(S5) Kohlbrecher, J.; Bressler, I. SASfit. 2011, version 0.93.3; `http://kur.web.psi.ch/sans1/SANSSoft/sasfit.html`.

(S6) Kohlbrecher, J. SASfit: A program for fitting simple structural models to small angle scattering data. Paul Scherrer Institute, 2012.